Anselmino, Matteo; Torri, Federica; Ferraris, Federico; Calò, Leonardo; Castagno, Davide; Gili, Sebastiano; Rovera, Chiara; Giustetto, Carla; Gaita, Fiorenzo. Anatomic relationship between left coronary artery and left atrium in patients undergoing atrial fibrillation ablation. JOURNAL OF CARDIOVASCULAR MEDICINE. 18 (7) pp: 528-533.
DOI: 10.2459/JCM.0000000000000484

Anatomic relationship between left coronary artery and left atrium in patients undergoing atrial fibrillation ablation

Matteo Anselmino*, Federica Torri†, Federico Ferraris*, Leonardo Calò‡,

Davide Castagno*, Sebastiano Gili*, Chiara Rovera*, Carla Giustetto*, Fiorenzo Gaita*

*Division of Cardiology, University of Torino, Department of Medical Sciences,

"Città della Salute e della Scienza" Hospital, Turin, Italy

†University of Cagliari, Dept. of Cardiovascular and Neurological Sciences, Monserrato /Italy

‡Division of Cardiology, Policlinico Casilino, ASL Rome, Italy

Corresponding Author:

Fiorenzo Gaita

Division of Cardiology, University of Torino

Department of Medical Sciences

"Città della Salute e della Scienza" Hospital

Corso A.M. Dogliotti, 14

10126 Torino, Italy

Phone 00 (39) 011 6709596 Fax 00 (39) 011 2369596

fiorenzo.gaita@unito.it

Abstract

Background Atrial fibrillation (AF) transcatheter ablation (TCA) is, within available AF rhythm control strategies, one of the most effective. In order to potentially improve ablation outcome in case of recurrent AF after a first procedure or in presence of structural myocardial disease, isolation of the pulmonary veins may be associated with extensive lesions within the left atrium (LA). To avoid rare, but potentially life-threatening complications thorough knowledge and assessment of LA anatomy and its relation to structures in close proximity is, therefore, mandatory. Aim of the present study is to describe, by cardiac Computed Tomography (CT), the anatomic relationship between aortic root, left coronary artery and LA in patients undergoing AF TCA.

Methods and Results The cardiac CT scan of 21 patients affected by AF was elaborated to segment LA, aortic root and left coronary artery from the surrounding structures and the following distances measured: LA and aortic root; LA roof and aortic root; left main coronary artery and LA; circumflex artery and LA appendage; circumflex artery and mitral valve annulus. Above all, the median distance between LA and aortic root (1.9, 1.5-2.1 mm), and between circumflex artery and LA appendage ostium (3.0, 2.1-3.4 mm) were minimal (≤ 3 mm). None of measured distances significantly varied between patients presenting paroxysmal versus persistent AF.

Conclusion The anatomic relationship within LA and coronary arteries is extremely relevant when performing AFTCA by extensive lesions. Therefore, at least in the latter case, pre-ablation imaging should be recommended to avoid rare, but potentially life-threatening complications with the aim of an as safe as possible procedure.

Introduction

Atrial Fibrillation (AF), the most prevalent sustained supraventricular arrhythmia[1], due to the combination of altered hemodynamics, atrioventricular dyssynchrony, and thromboembolic risk[2] relates to substantial morbidity and reduction in functional status and quality of life. Transcatheter ablation (TCA) is, within available AF rhythm control strategies, one of the most effective. Circumferential ablation of the pulmonary veins (PVs), obtaining electrical isolation, achieves in paroxysmal AF patients a freedom from the arrhythmia at 1 year of about 80%[3]. However, in case of persistent AF, freedom from relapses is significantly lower, stimulating continuous search of new AF triggers and mechanisms of maintenance, especially within the LA. In fact, complex AF TCA protocols including extensive linear lesions in the LA[3], ablation of fragmented atrial potentials[4], rotors and/or drives[5-6] and, eventually electrical isolation the LA appendage[7] are under investigation in case of redo ablation procedures and/or in presence of structural myocardial disease[8]. These approaches surely potentially improve the outcome of the procedure but, on the other side, should not increase the risk of rare but potentially life-threatening complications, such as atrial-esophageal fistula[8] or coronary artery damage[9]. To perform the safest procedure possible, in fact, before performing an AF TCA, thorough knowledge and assessment of LA anatomy and its relation to structures in close proximity is, in our opinion, mandatory.

Aim of the present study is to describe, by cardiac Computed Tomography (CT), the anatomic relationship between aortic root, left coronary artery and LA in patients undergoing AF TCA.

Methods

The study population included 25 consecutive patients with drug-refractory symptomatic AF undergoing TCA from June 2014 to May 2015, in whom pre-ablation cardiac CT was performed due to contraindications for Magnetic Resonance (e.g. claustrophobia, implanted cardioverter-defibrillator or cardiac pacemaker, metal prosthesis).

Image acquisition

Cardiac CT, that has a high spatial and temporal resolution[10-11-12-13], was performed by a 64 detector row (LightSpeed VCT, GE Health-care, Alexandria, Virginia) while 80 ml intravenous iodinated nonionic high concentration contrast was administered at the infusion rate of 5 ml/sec followed by a bolus of 60 ml of saline infusion at the infusion rate of 5 ml/sec. Slice acquisition thickness ranged from 0.625 to 1.25 mm and was electrocardiogram-gated, preferentially during inspiratory apnea. For all patients (both in sinus rhythm than in AF), to ensure imaging quality, a minimum of 70% of the frames with timing of acquisition in the diastole was required and reached in all cases.

The images generated by the CT scan were then integrated in the CARTO® 3 (Biosense Webster Inc., CA, USA) electroanatomical mapping system equipped with the latest image integration software (CARTOMERGE® Plus, Biosense Webster Inc., CA, USA). By a computerized algorithm differentiating the boundary between the blood pool (high in contrast) and the endocardium (which is not contrast-enhanced) the latter software permits a 3-D anatomic extraction process that segments the LA, aortic root and left coronary artery from the surrounding structures. The structure‘s volume was created using a set threshold intensity range defined manually, in order to better recognizes the different segments of interest. The segmented structures were subsequently individually extracted and rendered as 3-D surface reconstructions. When adequate segmentation was achieved, the surface images were stored in the CARTO® 3 system. The accuracy of this technique has been validated in animal studies[14-15].

In 4 patients (4/25, 16%), despite standard image acquisition, the left coronary artery was not clearly contrasted; these patients were therefore excluded from further analysis.

Anatomy Definitions

The ostium of a structure has been defined as the point in which the structure is flexed into another: e.g. the LA appendage ostium is the point in which the left appendage is flexed into the LA, the left main coronary artery ostium is the point in which the vessel is flexed into the aorta.

The LA is considered as having four walls (postero-superior or posterior, septal, anterior and lateral). The appendage ostium was divided in 4 sections: infero-anterior, supero-anterior, supero-lateral, and infero-lateral. Moreover the circumflex artery portion encircling the LA appendage was defined as "proximal".

Measurements

The surface images, stored in the CARTO® 3 system, were then integrate in CARTOMERGE® Plus software (Biosense Webster Inc., Diamond Bar, CA, USA). In this latter software, we used a transparent plane (clipping plane) to cut out segments of the 3D surface reconstructions to better understand highlight points of interest. By this technique the following distances were measured, exclusively based on the processed cardiac CT scans:

- LA - aortic root: a sagittal clipping plane (plane A) positioned on the LA, scanned for the minimum distance between any portion of the LA and the aortic root, by moving this plane from the left to the right LA (Figure 1).

- LA roof line - aortic root: the roof line was defined as the most anterior line, on the upper portion of the LA, connecting the ostium of the two superior PVs. A clipping plane (plane B) was placed parallel to the left superior PV ostium and then moved from the left to the right side of the LA to measure maximum and minimum distance from the roof line described above and the closest

portion of the aortic root. In order to ensure that the distance was measured on the same spatial plane, it was always computed parallel to plane B.

- Left main coronary artery - LA: a sagittal clipping plane (plane C) located on the LA, was moved to scan for the minimum distance between the left main coronary artery ostium and any portion of the LA (Figure 2).

- Circumflex artery (CX) – LA appendage: a clipping plane (plane D) was located parallel to the LA appendage ostium and was measured the distance between the LA appendage ostium and the circumflex artery (CX – LA appendage ostium; Figure 3). The plane D was then moved along the long axis of the LA appendage in search of the minimum absolute distance between the appendage and the artery (CX - LA appendage min).

- Mitral annulus- CX: a clipping plane (plane E) was placed parallel to the mitral annulus and then moved along a perpendicular axis of the mitral annulus in search of the minimum distance between the proximal CX and the mitral annulus. In order to ensure that the distance was measured on the same spatial plane it was always drawn parallel to plane E.

Statistical analysis

Continuous variables are expressed as median with lower and upper quartiles (Q1-Q3) and categorical variables as percentages. Continuous variables were compared between strata by means of Wilcoxon-Mann-Whitney test, and categorical variables in two-way tables by means of the Fisher exact test. A two sided p-value <0.05 was considered statistically significant and all analyses were performed with SPSS 20.0 (SPSS Inc, Chicago, IL, USA).

Results

Clinical characteristics of the 21 patients (90% males; median age 63 years) enrolled in the study are listed in Table 1. Median radiation exposure due to the cardiac CT was 752 (613-1045) mGy/cm; 8 (38%) patients performed the CT scan during persistent AF.

Twenty (95%) patients had a left main coronary artery originating from the left aortic sinus of Valsalva while one (5%) presented a separate origin of the left anterior descending and CX coronary arteries from the left aortic sinus of Valsalva. A classical left coronary branching of the left anterior descending and CX coronary arteries was present in 16 (76%) patients, while 5 (24%) patients had an intermediate coronary artery.

The relative distances between aortic root, left coronary artery and LA are summarized in Table 2, also stratified by type of AF.

Above all, the median distance between the LA and the aortic root, and the distance within CX and the LA appendage ostium were minimal (≤ 3 mm). Moreover, the minimum CX – LA left appendage distance was localized in the infero-anterior section of the LA left appendage ostium in 17 (81%) patients, while in the infero-lateral (directed towards the infero-anterior) in the remaining 4 (19%).

None of measured distances significantly varied between patients presenting paroxysmal versus persistent AF.

Discussion

Pre-ablation cardiac CT assessing the anatomic relationship between the LA and the left coronary artery, highlighted the close proximity of the LA to the left coronary artery. The use of an electroanatomical mapping system, as that used in the present study, permitting integration of the 3D CT reconstruction in the virtual navigation and ablation, therefore candidates as an extremely useful method to avoid/limit rare, but potentially life-threating complications during AF TCA.

The primary clinical benefit of AF TCA is quality of life improvement, deriving from elimination of arrhythmia-related symptoms such as palpitations, fatigue or effort intolerance. Unfortunately, the procedure is not always successful and exposes the patient to a 0.8-5.2%[16] risk of complications such as those at the vascular system, PV stenosis, phrenic nerve paralysis, cardiac tamponade, and thromboembolic events. In fact, circumferential PV isolation, permits to eliminate paroxysmal AF in about 80% of the cases[17], but the performance is indeed worst in patients with persistent and longstanding persistent AF. For this reason, additive ablation strategies are commonly investigated: the most common strategies, to date, include the creation of atrial linear lesions[3], ablation of rotors and drivers[5-6], Complex Fractionated Atrial Electrograms (CFAEs)[4], ganglionated plexi[18], and isolation of other non PV Triggers, as the coronary sinus or the LA appendage[3]. More in details, common atrial linear lesion performed are the following: the LA "roof" line, connecting the superior aspects of the left and right upper PVs; the "mitral isthmus" line, connecting the region of tissue between the mitral annulus and the left inferior PV; and the "anterior" line, connecting the roof line to the mitral annulus[19]. These lesions hold the potential to improve AF TCA outcome, however, need to be performed with thorough knowledge of LA anatomy to limit the risk of rare, but potentially life-threatening complications, such as atrial-esophageal fistula or coronary artery damage.

By CT coronary angiograms, Walsh et al.[20] reported that the left main coronary artery is intimately related to the anterior LA, LA appendage ostium, pulmonary artery and occasionally to the inferior portion of the left aortic sinus of Valsalva. Radiofrequency (RF) ablation in the LA may, therefore,

in case of close proximity, potentially harm this coronary artery. This complication, indeed, has been reported in 0.2-1.3% of the cases of ablation of accessory pathways[21], in which injury of coronary arteries have been described due to direct RF thermal injury causing spasm and/or oedema of the arterial wall. Injury of the coronary arteries, in addition, does not seem related to underlying vascular disease or predisposition given that Schneider et al. also described two cases (0.9% of their dataset) of acute coronary artery occlusion in infants, immediately after catheter ablation of a postero-septal accessory pathway[22].

In addition, indifferently from the goal (e.g. accessory pathway, AF or ectopic activity), the coronary sinus (CS) represents a high-risk ablation site due to its close proximity to the CX. In vivo topographic anatomy performed by selective coronary angiography or CT, demonstrated the narrow space, in 30-50% of the cases below 5 mm, between the coronary arteries (CX or posterolateral branch of the right coronary artery) and the ostium of the CS[23]. Eventually also right sided transcatheter ablation may harm the coronary arteries. Following cavo-tricuspidal isthmus ablation for common atrial flutter, in fact, injury to the RCA has been reported[24].

More specifically related to AF TCA, instead, reports are emerging only recently. Following "mitral isthmus" linear ablation an acute CX occlusion[25] and a fistula to the LA[26] have been reported. Moreover, a case of reversible sinus node dysfunction has been reported following an ablation performed between LA appendage and left superior PV that injured the sinus nodal artery originating from the left circumflex artery[27].

The CX lies in the epicardium of the atrioventricular groove and is in close proximity to the CS and the LA endocardium at the level of the mitral isthmus. The distances between the LA and the aortic root, and the distances within CX and the LA appendage ostium and mitral annulus registered in the present study appear, indeed, narrow (median $\leq$ 3 mm). In support of a previous study[9] suggesting that the risk of CX injury during ablation of the mitral isthmus is increased when performed in a more 'distal' region in respect to a catheter reference inside the coronary sinus, in the present study

the minimum CX – LA distance was localized in the infero-anterior section of the LA appendage ostium the majority (81%) of patients.

In this setting, before radiofrequency (RF) energy is delivered[28], thorough knowledge and assessment of LA anatomy and its relation to structures in close proximity seems essential. Ablation lesions created by RF can reach about 5 mm in depth, especially in case of use of active electrode cooling, as for AF TCA despite small electrodes at relatively low power[29]. In addition, pre-clinical and clinical studies indicate that electrode-tissue contact force[30] is a main determinant of RF lesion size and depth. In fact, no effective lesion is formed without adequate contact force, while excessive contact force is associated with unnecessary deep tissue heating and increased risk of steam pop (and perforation) involving structures in close proximity to the LA. The LA wall is thin, commonly about 5 mm; in particular, however, the anterior wall measures an average of 2 mm in the area near the vestibule, and the posterior and lateral walls are between 3 and 6 mm[31].

In conclusion, it is reasonable that every structure in proximity to the LA (<5 mm) may be damaged by a RF application, including the left coronary artery. On the other side, few factors may potentially limit these dramatic complications. Not only the fat tissue surrounding the artery could have protective effects, but also the blood flow in the vessel tends to prevent from an increase in temperature by convective cooling[25]. However, concerning the latter aspect, computer models have suggested that circulating blood flow has little effect on the subsequent temperature effects on adjacent tissue[32-33]. In fact, it is known that late gadolinium enhancement at the descending aorta wall was increased among patients undergoing transcatheter RF PVI[34]. Moreover, a potential cooling effect may also be reduced in the presence of coronary atherosclerotic disease, which facilitates thrombus formation in the coronary arteries[35] hence, supporting the evidence, that when this cardiovascular structure is close to the RF points delivery, there is a potential situation of risk.

Limitations

As the limited sample of patients examined, we could not have found rare anatomic variants. In addition, although the CT scans were acquired with breath held during ventricular diastole, cardiac gating may result challenging during AF, (present in about a third of patients in the present dataset), not guarantying that 100% of the frames acquired were performed at the same cardiac cycle time. Eventually, RF energy during AF TCA is applied continuously throughout the cardiac and respiratory cycles; the considerable flexibility and movement of the anterior LA and of the other structures during these cycles could potentially modify the distances between each other's. During segmentation, the threshold intensity range was manually set, and could have determined variation in the dimension of the anatomical structures.

Conclusion

The present study highlights the proximity of the coronary arteries to common RF delivery sites during AF TCA, emphasizing the potential for serious complications. Although clinically manifest coronary injury is extremely low, it is a know complication. Pre-ablation imaging should therefore be considered to guide tailored RF application (duration, temperature and contact force) on specific patient's anatomy.

Figures legend

Figure 1. Measurement of the distance on plane A, sagittal to the left atrium, between the aortic root and the first portion of the left atrium. In this example the LA - aortic root distance resulted less than 1 mm.

Figure 2. Measurement of the distance on plane C, sagittal to the left atrium, between the left main coronary artery ostium (LMCA) and the first portion of the left atrium (LA). In this example the Left main coronary artery - LA distance resulted less than 4 mm.

Figure 3. Measurement of the distance on plane D, parallel to the left atrium appendage ostium, between the left atrium appendage ostium and the circumflex artery. In this example the CX – LA appendage distance was of 2.1 mm.

Table 1. Clinical characteristics of the study population. Data are expressed as medians with lower and upper quartiles if not differently stated. AF, atrial fibrillation.

Variable	**n=21**
Age (years)	63 (59-69)
Male/Female (%)	19 (90.5%)
Body Mass Index (Kg/m²)	26.4 (24.1-28.8)
Type of Atrial Fibrillation (%)	
Paroxysmal	13 (61.9%)
Persistent	8 (38.1%)
Duration of AF (years)	6 (5-48)
Known heart diseases (%)	
Coronary heart disease	0
Dilated cardiomyopathy	2 (9.5%)
Hypertrophic cardiomyopathy	0
Valvular heart disease	4 (19.0%)
Hypertension (%)	8 (38.1%)
Left ventricular ejection fraction (%)	60 (57-64)

Table 2. Distances between aortic root, left coronary artery and LA stratified by type of atrial fibrillation. Values reported in millimeters and expressed as medians with lower and upper quartiles (within brackets).

Variable	ALL (n=21)	Paroxysmal (n=13)	Persistent (n=8)	P value
	Median (Q1-Q3)	Median (Q1-Q3)	Median (Q1-Q3)	
LA roof line - aortic root max	35.7 (31.1-40.7)	32.9 (28.6-38.7)	36.3 (33.2-44.3)	0.11
LA roof line - aortic root min	28.5 (23.5-32.8)	28.3 (21.6-32.2)	28.7 (23.7-32.8)	0.68
LA - aortic root	1.9 (1.5-2.1)	1.7 (1.5-2.4)	2.0 (1.9-2.1)	0.24
Left main coronary artery - LA	5.8 (3.8-8.9)	5.9 (3.2-9.3)	5.6 (4.0-8.7)	0.99
CX – LA appendage ostium	3.0 (2.1-3.4)	3.2 (2.3-4.1)	2.9 (1.9-3.2)	0.37
CX-LA appendage min	2.5 (1.9-3.4)	2.5 (2.1-3.3)	2.3 (1.5-3.5)	0.92
Mitral anulus-CX	3.6 (2.7-6.2)	4.0 (3.0-5.8)	2.8 (1.3-5.7)	0.38

5

References

1. Andrade J, Khairy P, Dobrev D, Nattel S. The clinical profile and pathophysiology of atrial fibrillation relationships among clinical features, epidemiology, and mechanisms. Circ Res 2014; 114:1453-1456.
2. Anselmino M, Scaglione M, Di Biase L, Gili S, Santangeli P, Corsinovi L, Pianelli M, et al. Left atrial appendage morphology and silent cerebral ischemia in patients with atrial fibrillation. Heart Rhythm 2014; 11 (1):2-7.
3. Raviele A, Natale A, Calkins H, Camm JA, Cappato R, Ann Chen S, Connolly SJ et al. Venice chart international consensus document on atrial fibrillation ablation: 2011 update. J Cardiovasc Electrophysiol 2012; 23:890-923.
4. Nademanee K, Schwab M, Porath J, Abbo A. How to perform electrogram-guided atrial fibrillation ablation. Heart Rhythm 2006; 3:981-4.
5. Ryu K, Shroff SC, Sahadevan J, Martovitz NL, Khrestian CM, Stambler BS. Mapping of atrial activation during sustained atrial fibrillation in dogs with rapid ventricular pacing induced heart failure: evidence for a role of driver regions. J Cardiovasc Electrophysiol 2005;16:1348-58.
6. Shivkumar K, Ellenbogen KA, Hummel JD, Miller JM, Steinberg JS. Acute termination of human atrial fibrillation by identification and catheter ablation of localized rotors and sources: first multicenter experience of focal impulse and rotor modulation (FIRM) ablation. J Cardiovasc Electrophysiol 2012;23:1277-85.
7. Di Biase L, Burkhardt JD, Mohanty P, Sanchez J, Mohanty S, Horton R, Gallinghouse GJ et al. Left atrial appendage: an underrecognized trigger site of atrial fibrillation. Circulation 2010; 122:109-1.

8. Kirchhof P, Benussi S, Kotecha D, Ahlsson A, Atar D, Casadei B, Castella M, et al. 2016 ESC Guidelines for the management of atrial fibrillation developed in collaboration with EACTS: The Task Force for the management of atrial fibrillation of the European Society of Cardiology (ESC)Developed with the special contribution of the European Heart Rhythm Association (EHRA) of the ESCEndorsed by the European Stroke Organisation (ESO). Europace 2016 Aug 27. pii: euw295 [Epub ahead of print]
9. Wittkampf FH, van Oosterhout MF, Loh P, Derksen R, Vonken EJ, Slootweg PJ, Ho SY. Where to draw the mitral isthmus line in catheter ablation of atrial fibrillation: histological analysis. Eur Heart J 2005; 26:689-95.
10. Choure AJ, GarciaMJ, Hesse B, Sevensma M, Maly G, Greenberg NL, Borzi L et al. In vivo analysis of the anatomical relationship of coronary sinus to mitral annulus and left circumflex coronary artery using cardiac multidetector computed tomography: implications for percutaneous coronary sinus mitral annuloplasty. J Am Coll Cardiol 2006;48:1938–45.
11. Tops LF, Van de Veire NR, Schuijf JD, de Roos A, van der Wall EE, Schalij MJ, Bax JJ. Noninvasive evaluation of coronary sinus anatomy and its relation to the mitral valve annulus: implications for percutaneous mitral annuloplasty. Circulation 2007;115:1426–32.
12. Jongbloed MR, Lamb HJ, Bax JJ, Schuijf JD, de Roos A, van der Wall EE, Schalij MJ. Noninvasive visualization of the cardiac venous system using multislice computed tomography. J Am Coll Cardiol 2005;45:749–53.
13. Van de Veire NR, Schuijf JD, De Sutter J, Devos D, Bleeker GB, de Roos A, van der Wall EE et al. Non-invasive visualization of the cardiac venous system in coronary artery disease patients using 64-slice computed tomography. J Am Coll Cardiol 2006;48:1832–8.
14. Dickfeld T, Dong J, Solomon SB, Lardo AC, Berger R, Halperin H, Calkins H. Assessment of position error of catheter mapping system (Biosense Carto V8) with CT/MR image integration capabilities. Heart Rhythm 2005;2:S278.

15. De Ponti R, Salerno-Uriarte JA. Non-fluoroscopic mapping systems for electrophysiology: the 'tool or toy' dilemma after 10 years. Eur Heart J 2006; 27(10):1134-6.

16. Baman TS, Jongnarangsin K, Chugh A, Suwanagool A, Guiot A, Madenci A, Walsh S et al. Prevalence and predictors of complications of radiofrequency catheter ablation for atrial fibrillation. J Cardiovasc Electrophysiol 2011; 22:626-31.

17. Bhargava M, Di Biase L, Mohanty P, Prasad S, Martin DO, Williams-Andrews M, Wazni OM et al. Impact of type of atrial fibrillation and repeat catheter ablation on long-term freedom from atrial fibrillation: results from a multicenter trial. Heart Rhythm 2009; 6:1403-12.

18. Kurotobi T, Shimada Y, Kino N, Ito K, Tonomura D, Yano K, Tanaka C et al. Features of intrinsic ganglionated plexi in both atria after extensive pulmonary isolation and their clinical significance after catheter ablation in patients with atrial fibrillation. Heart Rhythm. 2015 Mar;12(3):470-6.

19. Gaita F, Caponi D, Scaglione M, Montefusco A, Corleto A, Di Monte F, Coin D, et al. Long-term clinical results of 2 different ablation strategies in patients with paroxysmal and persistent atrial fibrillation. Circ Arrhythm Electrophysiol. 2008 Oct;1(4):269-75.

20. Walsh KA, Fahy GJ. Anatomy of the left main coronary artery of particular relevance to ablation of left atrial and outflowtract arrhythmias. Heart Rhythm 2014; 11:2231-38.

21. Solomon AJ, Tracy CM, Swartz JF, Reagan KM, Karasik PE, Fletcher RD. Effect on coronary artery anatomy of radiofrequency catheter ablation of atrial insertion sites of accessory pathways. J Am Coll Cardiol 1993; 21:1440-4.

22. Schneider HE, Kriebel T, Gravenhorst VD, Paul T. Incidence of coronary artery injury immediately after catheter ablation for supraventricular tachycardias in infants and children. Heart Rhythm 2009; 6:461-7.

23. Mao J, Moriarty JM, Mandapati R, Boyle NG, Shivkumar K, Vaseghi M. Catheter ablation of accessory pathways near the coronary sinus: value of defining coronary arterial anatomy. Heart Rhythm 2015; 12:508-14.

24. Al Aloul B, Sigurdsson G, Adabag S, Li JM, Dykoski R, Tholakanahalli VN. Atrial flutter ablation and risk of right coronary artery injury. J Clin Med Res. 2015 Apr;7(4):270-3.

25. Takahashi Y, Jais P, Hocini M, Sanders P, Rotter M, Rostock T, et al. Acute occlusion of the left circumflex coronary artery during mitral isthmus linear ablation. J Cardiovasc Electrophysiol 2005; 16:1104-7.

26. Hsieh CHC, O'Connor S, Ross DL. Circumflex coronary artery to left atrium fistula caused by mitral isthmus ablation. Heart, Lung and Circulation 2014; 23, 689-92.

27. Choi EK, Lee W, Oh S. Reversible sinus node dysfunction after multiple ablations along the course of sinus nodal artery in patient with paroxysmal atrial fibrillation. Europace. 2013 Oct;15(10):1388.

28. Demaria RG, Pagé P, Leung TK, Dubuc M, Malo O, Carrier M, Perrault LP. Surgical radiofrequency ablation induces coronary endothelial dysfunction in porcine coronary arteries. Eur J Cardiothorac Surg 2003;23:277–282.

29. Yokoyama K, Nakagawa H, Shah DC, Lambert H, Leo G, Aeby N, Ikeda A et al. Novel contact force sensor incorporated in irrigated radiofrequency ablation catheter predicts lesion size and incidence of steam pop and thrombus. Circ Arrhythmia Electrophysiol 2008; 1:354-62.

30. Stabile G, Solimene F, Calò L, Anselmino M, Castro A, Pratola C, Golia P, et al. Catheter-tissue contact force values do not impact mid-term clinical outcome following pulmonary vein isolation in patients with paroxysmal atrial fibrillation. J Interv Card Electrophysiol. 2015 Jan;42(1):21-6.

31. Ho SY, Sanchez-Quintana D, Cabrera JA, Anderson RH. Anatomy of the left atrium: implications for radiofrequency ablation of atrial fibrillation. J Cardiovasc Electrophysiol 1999; 10:1525-33.

32. Berjano EJ, Hornero F. What affects esophageal injury during radiofrequency ablation of the left atrium? An engineering study based on finite-element analysis. Physiol Meas 2005;26:837–848.

33. Hornero F, Berjano EJ. Esophageal temperature during radiofrequency-catheter ablation of left atrium: a three-dimensional computer modeling study. J Cardiovasc Electrophysiol 2006;17:405–410.

34. Tung P, Hong SN, Chan RH, Peters DC, Hauser TH, Manning WJ, Josephson ME. Aortic injury is common following pulmonary vein isolation. Heart Rhythm 2013; 10:653-58.

35. Wong KC, Sadarmin PP, Prendergast BD, Betts TR. Acute occlusion of left circumflex artery following radiofrequency catheter ablation at the mitral isthmus. Europace 2010;12:743–5.

Figure 1.

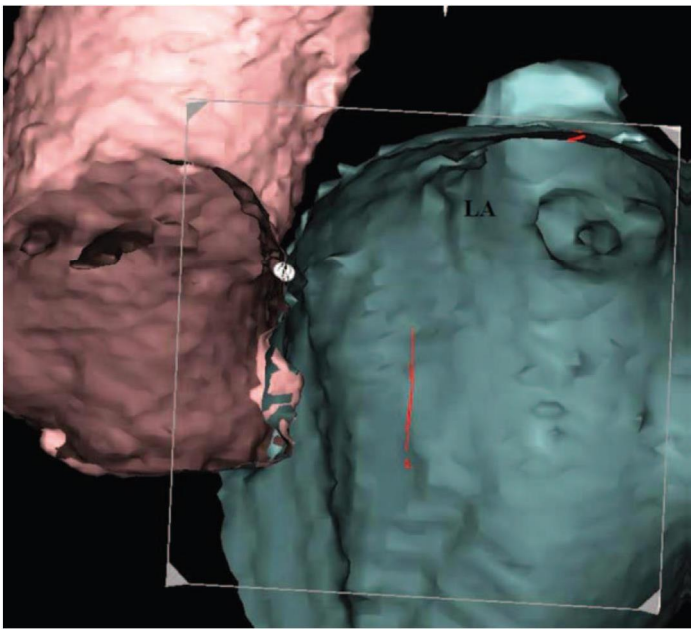

Figure 2.

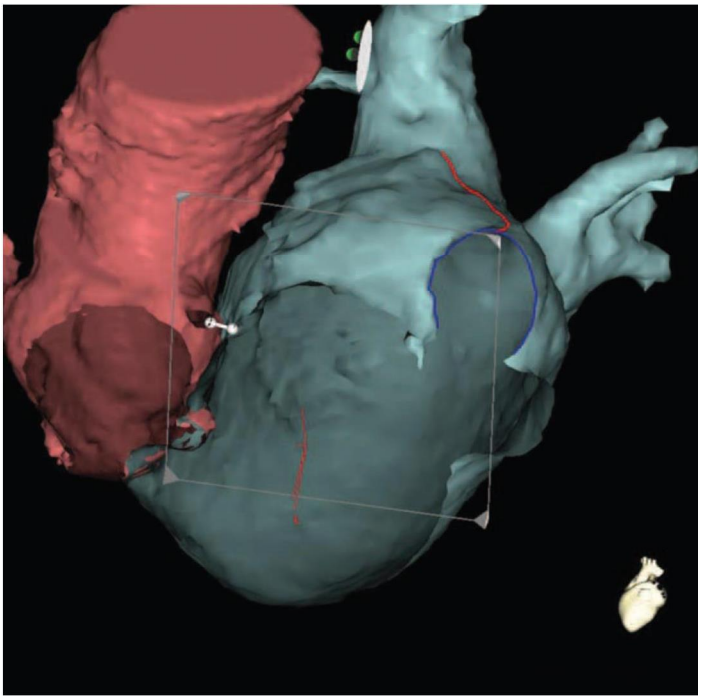

Figure 3.